Al-Qadisiyah Journal of Pure Science

ISSN(Printed): 1997-2490 ISSN(Online): 2411-3514

DOI: 10.29350/jops

Al-Qadisiyah Journal of Pure Science

Tuning optoelectronic and thermodynamic properties of coupled dinuclear complexes

Asmaa Obais Radhi[1], Qusiy H. Al-Galiby[2]

Received: 27/03/2026; Revised: 09/04/2026; Accepted: 14/04/2026; Published Online: 14/04/2026.

Abstract

Understanding how coordinated metal ions regulate electronic structure is crucial for the rational design of functional optoelectronic materials. In this study, we investigated the role of metal identity in controlling the optoelectronic properties of two coupled metal centres incorporating Co, Cu, Fe, Ni, Pt, Ru, and Zn within a unified coordination framework. Density functional theory (DFT) was performed using the B3LYP functional with the LanL2DZ basis set to elucidate structure–property relationships. The results reveal that substitution of the coordinated metal centre enables systematic tuning of the frontier molecular orbitals, leading to significant modulation of the HOMO–LUMO energy gap. The resulting of dinuclear complexes show that the largest HOMO-LUMO energy gap was obtained for Co (E_g = 2.06 eV) and the smallest gap for Ni (E_g = 0.27 eV), supporting by the highest hardness (η = 1.03) for Co and the lowest hardness (η = 0.13) for Ni, indicating the highest stability and reactivity. The thermodynamic calculation reveals the negative magnitude of Gibbs free energies (ΔG) and interaction energies (ΔE_{int}) for all dinuclear complexes and range from -4.31 eV and -3.65 eV for Cu to -9.96 eV and -8.96 eV for Pt, respectively, confirming spontaneous formation and thermodynamic favorability, with the Pt atom-containing complex displaying the highest stability among the series. In the presence of the counter ion Cl^-, the interaction and Gibbs free energies for the iron-based complex (Fe-Cl) change from −8.31 eV and −7.58 eV to −24.45 eV and −24.23 eV, which shows a strong improvement in thermodynamic stability. Time-dependent TD-DFT calculations of the UV spectra indicate that all complexes exhibit absorption bands spanning the visible to near-infrared regions, highlighting their potential applicability in light-harvesting and

photonic devices. The findings demonstrate that the coordinated metal ion plays a decisive role in governing both the electronic structure and stability of dinuclear complexes. This work provides theoretical design guidelines for tailoring optoelectronic properties through strategic metal selection in coupled metal-centre systems.

Keywords
Dinuclear compounds, TD-DFT, optoelectronic properties, and electronic properties. Thermodynamic analysis.

1. Introduction

Organometallic complexes with multifunctional conjugated ligands have attracted significant attention due to their unique electronic, optical, and redox properties. Ligands with extended π-conjugation, containing both electron-donating and electron-withdrawing atoms, improve coordination chemistry and allow tuning of the physical properties of metal complexes for molecular-scale devices [1-5].

As an example of single host ligands, porphyrins have received particular attention due to their unique electronic and coordination properties. In organometallic chemistry, porphyrins are a well-known type of conjugated macrocyclic ligands that are often used as molecular host [6]. Effective electron delocalization is made possible by their highly conjugated π-system, and strong and specific coordination with transition metal ions is made possible by the central cavity created by four nitrogen atoms [7]. Porphyrins are perfect scaffolds for creating mononuclear and multinuclear metal complexes because of their strong coordination ability and electrical flexibility. Porphyrin-based systems, which exhibit tunable optical, electronic, and redox properties based on the selection of metal center and peripheral substitution patterns, have been thoroughly studied for applications in catalysis, photodynamic therapy, organic photovoltaics, and molecular electronics [8, 9].

Another example of single host was given by 4,4-difluorobenzhydryl groups into symmetrical-diimino-nickel catalysts, which significantly enhances their performance for ethylene polymerization, enabling the synthesis of high molecular weight polyethylene (PE) elastomers [10]. Although extensive research has been

conducted on mononuclear complexes using common molecular hosts including terpyridines, phthalocyanines, and porphyrins, a systematic understanding of how multiple metal centers affect optical and electrical properties is still missing. Most studies have focused on single-metal systems, therefore the effects of cooperative behavior and metal–metal interactions in dinuclear complexes are mainly unstudied [11-13]. However, this study addresses this gap by investigating dinuclear complexes, where two metal centers are coordinated within a single ligand framework, providing additional degrees of freedom to modulate frontier molecular orbitals, charge transfer efficiency, and thermodynamic stability [14].

This study focuses on the fluorinated ligand $C_{38}H_{20}N_4O_6F_{12}S_2$, which is rich in nitrogen and sulfur and provides multiple coordination sites (N, O, S), along with electronegative fluorine atoms that influence electronic distribution. It forms stable dinuclear complexes with divalent metal ions such as Co^{2+}, Cu^{2+}, Fe^{2+}, Ni^{2+}, Pt^{2+},Ru^{2+} and Zn^{2+} exhibiting diverse electrical and magnetic properties suitable for spin filters, molecular switches, and molecular wires [15].The electronic and optoelectronic properties were analyzed using Density Functional Theory (DFT) and Time-Dependent DFT (TD-DFT), evaluating HOMO–LUMO gaps, charge distribution, UV–Vis absorption spectra, and singlet–triplet energy differences [16]. Variations in the central metal ion significantly affect the frontier orbital energies, optical transition positions, magnetic stability, and energetic stability of the complexes [17]. Metal–ligand interaction strength and thermodynamic spontaneity were assessed via interaction energies and Gibbs free energy calculations, while the effect of auxiliary ligands, such as chloride ions in iron-based complexes, was also considered [18, 19]. These results highlight the crucial role of metal-ligand interactions in controlling molecular behavior and suggest potential applications in molecular spintronics, organic photovoltaics, electrochemical sensors, and nanoscale semiconductors [20, 21].

From the point of view of controlling and optimising optoelectronic and thermodynamic properties, molecular designed with coupled dinuclear complexes are of interest, because by varying the metal atom residing in the two hosts of the organic framework, it should be possible to tune the molecular energy levels of complex. In what follows, we shall demonstrate that this is indeed the case and that high optical, electrical and thermodynamic stability are achievable.

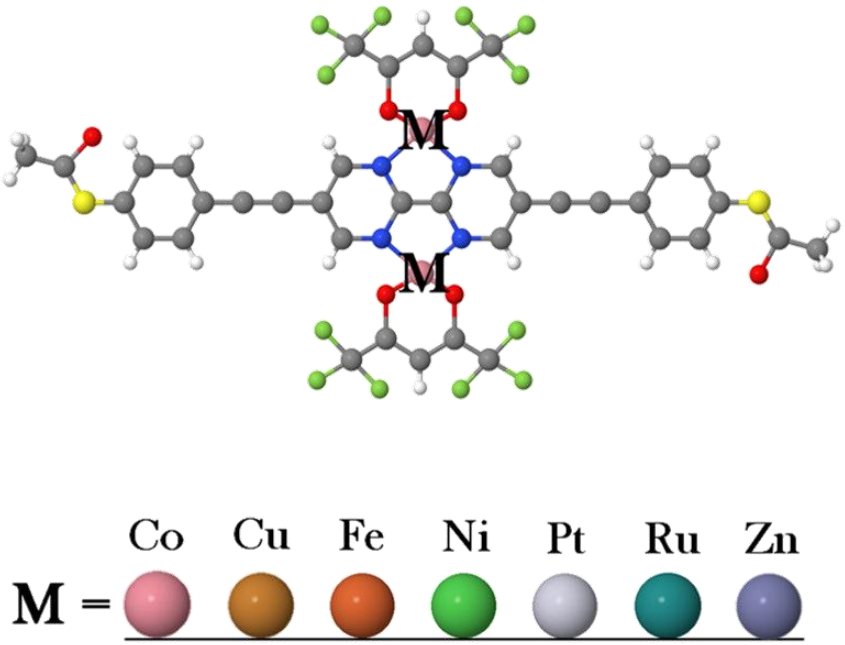

Figure 1: Chemical structure of dinuclear metal complexes ($C_{38}H_{20}N_4O_6F_{12}S_2$) with varied transmission metals Co^{2+}, Cu^{2+}, Fe^{2+}, Ni^{2+}, Pt^{2+}, Ru^{2+}, and Zn^{2+}.

2. Computational Method

To compute the optical and electronic properties of dinuclear metal complexes shown in Figure 1, the following method was performed. First the optimized geometry of molecule was found using the density functional theory (DFT), which implemented by Gaussian package and employed the B3LYP hybrid functional with the LanL2DZ basis set in ground state [22]. For geometry optimization, we calculated the electronic properties, including the HOMO and LUMO energies, ionization potential (IP), electron affinity (EA), frontier molecular orbitals, density of states and dipole moments. The time-dependent (TD-DFT) was employed for modeling UV-Vis and IR absorption spectra. The IP and EA quantities were calculated by using the following equations [18, 23]:

$$IP = E^{+} - E^{0} \quad (1)$$

$$EA = E^{0} - E^{-} \quad (2)$$

where E^{0} ($E^{\mp}$) refers to the ground state energy of neutral (charged) molecule.

From the calculated HOMO and LUMO, the energy gap, electronegativity (χ), chemical potential (μ), global hardness (η), and global softness (S) were calculated as follows equations [24, 25]:

$$\chi = -(E_{LUMO} + E_{HOMO})/2 \quad (3)$$

$$\mu = -\chi \quad (4)$$

$$\eta = (E_{LUMO} - E_{HOMO})/2 \quad (5)$$

$$S = 1/\eta \quad (6)$$

Interaction energies and Gibbs free energies were calculated to assess the stability of dinuclear metal complexes. Due to the chemical connection of metal centers with O and F atoms, the complex was fragmented into a ligand fragment ($C_{28}H_{18}N_4O_2S_2$) and a metal fragment ($M_2(C_{10}H_2O_4F_{12})$) [26].

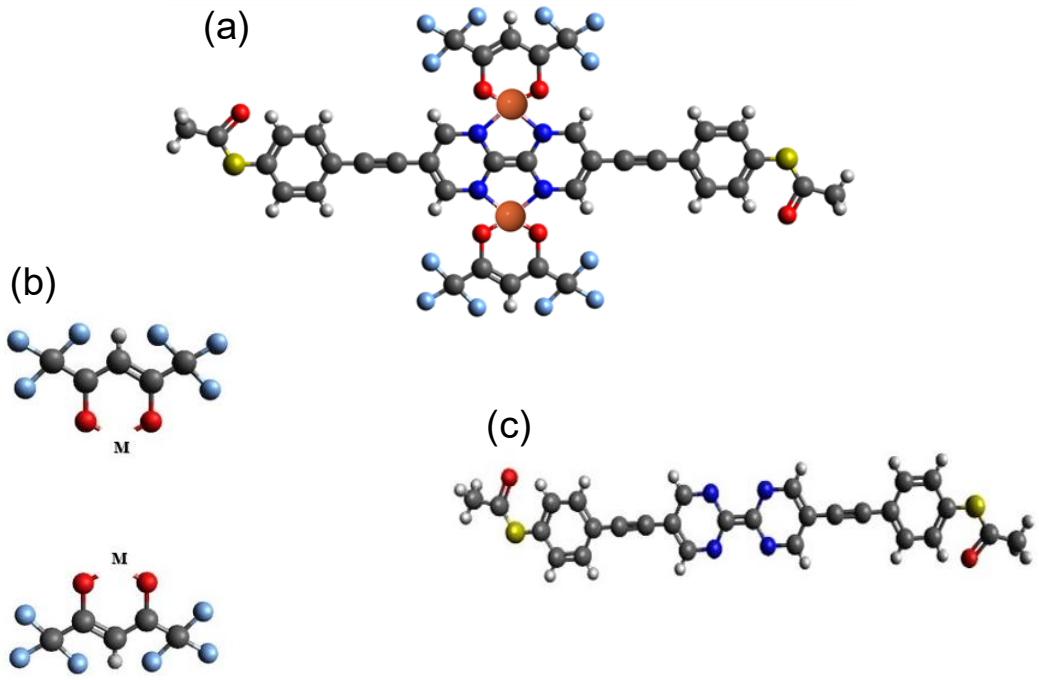

Figure 2: Molecular structures of complex, (a) the full optimized geometry with two metallic atoms. The metal ions (M^{+2}) are marked in green, oxygen in red, nitrogen in blue, carbon in grew, hydrogen in white, fullerene in silver and sulphur in yellow. (b) shows the coordination fullerene complex metal M. (c) the bare bipyrimidine wire based molecular structure.

The interaction energy is given by [27]:

$$\Delta E_{(Int+ZPE)} = E_{(complex)} - \left(E_{(Ligand)} + E_{(Metal)}\right) \quad (7)$$

The total electronic energy of the optimized dinuclear metal complex and the energies of the isolated ligand and metal ions were computed at the DFT/B3LYP/LanL2DZ level. Zero-point energy corrections were applied to obtain corrected interaction energies. Gibbs free energies (ΔG) were derived using vibrational frequencies at ideal geometries, factoring in thermal and entropic variables to accurately depict the coordination process during complex formation [28]:

$$\Delta G_{(bind)} = G_{(complex)} - \left(G_{(Ligand)} + G_{(Metal)}\right) \quad (8)$$

Additional computations for the iron complex Fe_2Cl_2 with coordinated chloride ions were performed to evaluate the effect of chloride coordination, using consistent theoretical and computational parameters for a realistic comparison [27, 29].

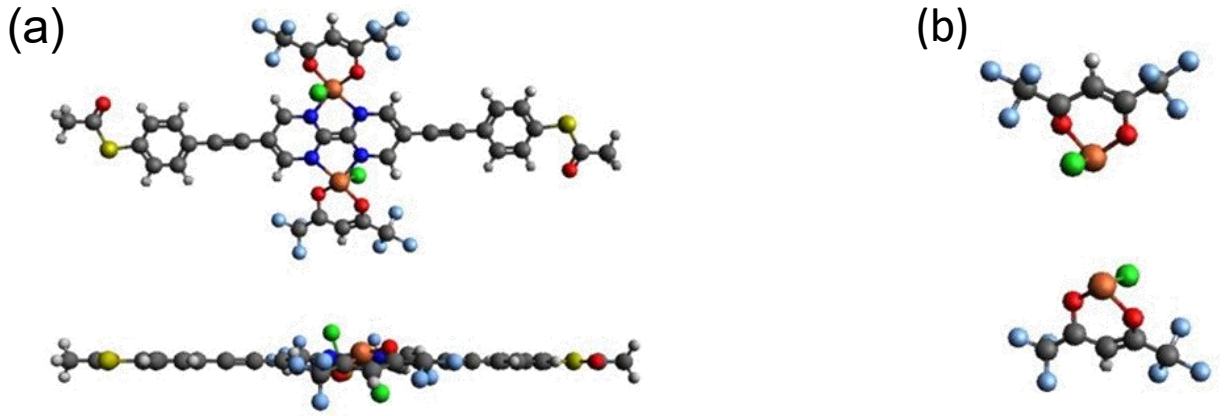

Figure 3: Optimized molecular structures of the studied systems: (a) the fully optimized dinuclear metal complex with Fe(III), which represented by Fe with counter ions Cl^-. (c) the optimized geometry of the isolated ligand complex.

3. Results and Discussions

3.1 Electronic properties

3.1.1 Electronic characteristics calculated using DFT

Table 1, Calculated the metallic molecules' HOMO, LUMO, ionization potential (IP), electron affinity (EA), energy gap (Eg), electronegativity (χ), chemical potential (μ), global hardness (η), and global softness (S).

Metal	HOMO(eV)	LUMO(eV)	Eg(eV)	χ	μ	η	S	IP(eV)	EA(eV)
Co	-5.91	-3.84	2.06	4.88	-4.88	1.03	0.96	6.20	2.91
Cu	-5.74	-3.98	1.75	4.86	-4.86	0.87	1.13	6.74	2.83
Fe	-6.30	-5.79	0.51	6.04	-6.04	0.25	3.90	3.78	7.78
Ni	-5.78	-5.51	0.27	5.65	-5.65	0.13	7.27	6.26	4.73
Pt	-5.74	-5.45	0.29	5.60	-5.60	0.14	6.79	6.70	4.96
Ru	-6.25	-5.76	0.48	6.01	-6.01	0.24	4.10	5.83	5.77
Zn	-4.62	-4.04	0.58	4.33	-4.33	0.29	3.43	5.71	2.92

The study analyzes the electronic parameters of various metal complexes using the DFT-B3LYP method. The cobalt (Co) complex displays the highest stability and the largest HOMO-LUMO energy gap (2.06 eV), while the nickel (Ni) complex shows the smallest gap (0.27 eV), indicating the highest reactivity. Copper (Cu) has the highest ionization potential (6.74 eV), suggesting it is less prone to oxidation, whereas iron (Fe) has the lowest potential (3.78 eV), indicating greater reactivity. The iron complex also has the highest electron affinity (7.78 eV) and electronegativity (6.04 eV), suggesting a strong tendency to accept electrons. The Co complex exhibits the highest thermodynamic stability and hardness (1.03 eV), while the Ni complex represents the most chemically active and soft system, making

it suitable for redox and catalytic applications. Conversely, Co stability suggests potential use in electronic materials.

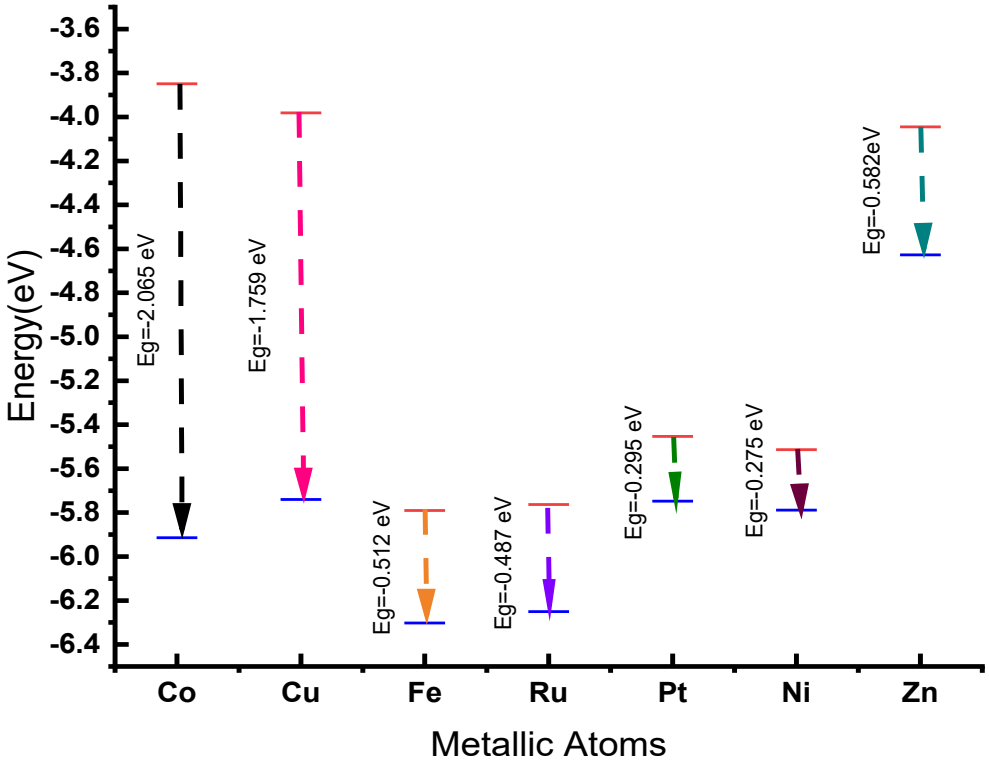

Figure 4: The complexes' computed electronic structure in DFT/B3LYP.

3.1.2 Orbitals of frontier molecules (FMOs)

Figure 5 illustrates the Frontier Molecular Orbitals (FMOs) of various transition metal complexes including Cobalt, Copper, Iron, Nickel, Platinum, Ruthenium, and Zinc. The Highest Occupied Molecular Orbitals (HOMO) and Lowest Unoccupied Molecular Orbitals (LUMO) reveal significant differences in electron density distribution. Complexes of Co, Cu, Fe, Pt, and Ru exhibit extensive electron delocalization indicating strong hybridization, while Ni and Zn complexes show pronounced electron localization. Notably, Zinc's filled d-orbital (d10) results in the HOMO being centered on the ligand rather than the metal. These distinctions are vital for understanding molecular traits such as oxidation-reduction potentials, spectroscopic properties, and catalytic activity, underscoring the importance of FMO analysis in developing materials with specific functionalities.

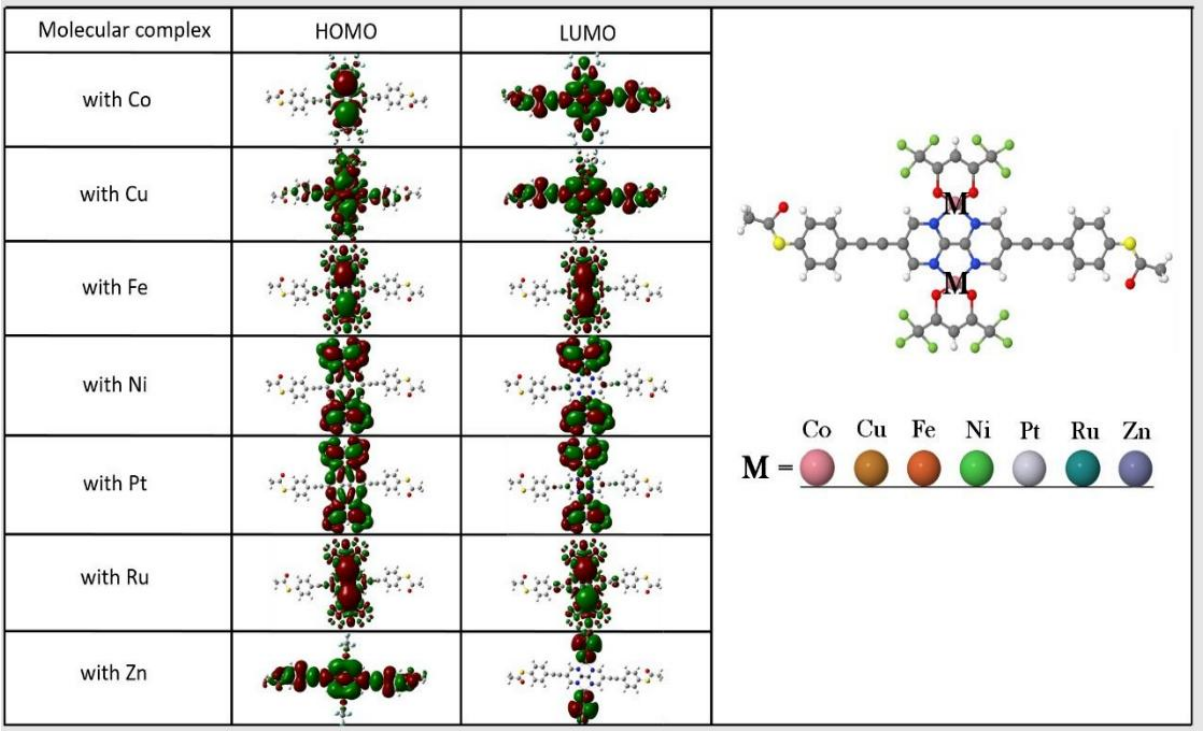

Figure 5: Frontier molecular orbitals (FMOs) of the metallo-molecules calculated using DFT/B3LYP.

3.1.3 Dipole moment effect

To explore how the electronic structures of these metals influence molecular geometry, reactivity, and physical properties, we calculated the dipole moment versus the varied transition metals, shown in Figure 6. The calculation shows that the larger magnitude of dipole moment was found in the case of Cu (4 Debye), which typically indicates to asymmetric geometry and the higher ionic character, due to a significant difference in electronegativity (strong charge transfer) between the metal and the ligands, leading to a more polarized bond. Whereas the smaller value of dipole moment was obtained in the case of Ni, indicating the high symmetry of molecule with Ni atom (1.8 Debye) and covalent character of bond between metal and ligands that share electrons more equally, resulting in less pull toward one end of the bond.

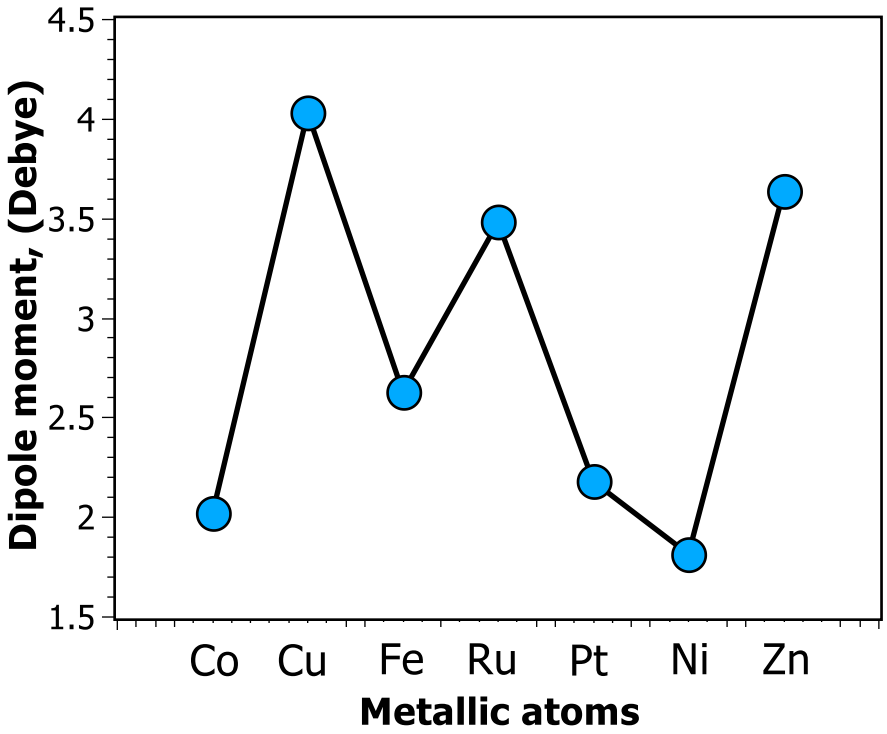

Figure 6. DFT calculation of dipole moment for each metallo-molecule.

3.1.4 Evaluation of Mulliken charges

To gain insights into how electrons are redistributed when different metals interact with ligands, we study the evaluation of Mulliken charges in molecules, involving various transition metals. Mulliken analysis quantifies the flow of electrons between ligands and the metal center, which is essential for identifying donor and acceptor atoms during complex formation. Herein, the DFT/B3LYP calculation demonstrate that among the list of metals the two metallic atoms Pt and Zn have the higher positively charged (stronger donor). The Pt atom can exhibit multiple, higher positive charges, including +2, +4 and +6 oxidation states, meaning its atoms can be more positively charged than Zn in certain environments. Whereas the Cu atom has a lower positive charge (+1), exhibiting a stable oxidation state compared to Co (+2) which reveals the lowest stable oxidation state. The Fe, Ni and Ru atoms exhibit intermediate complexes for donating electrons to the ligands host, as shown in Figure 7. These results predict that the influence of metal choice on the electronic environment, impacting chemical reactivity and stability in metallo-organic systems.

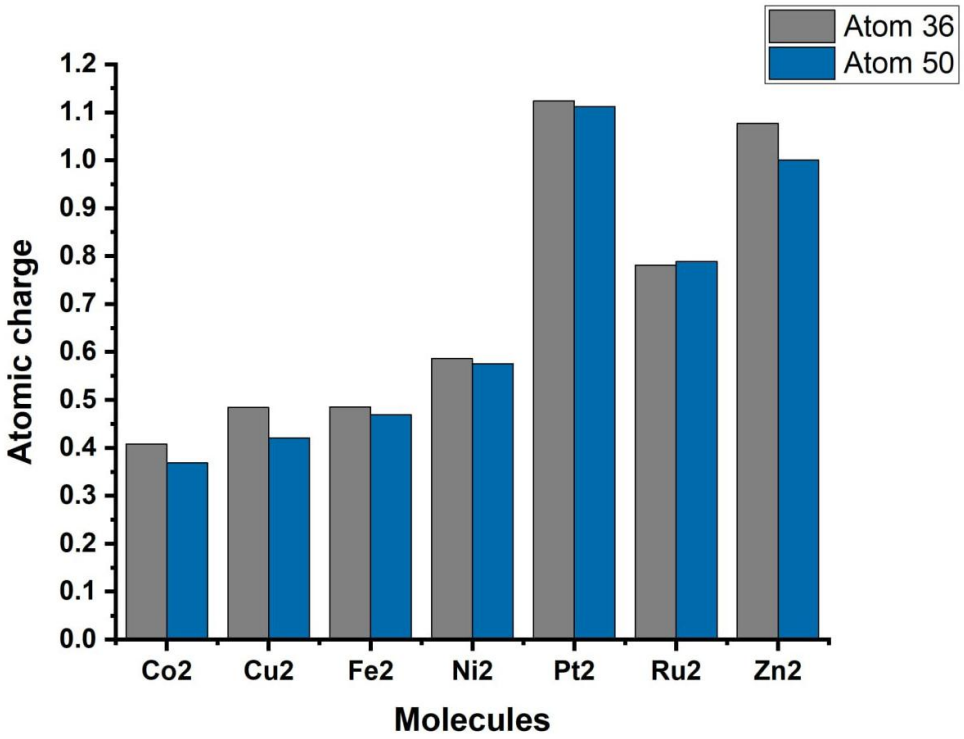

Figure 7: The Atomic charge of the molecules.

3.1.5 Density of states (DOS)

In this study, the density of states (DOS) and molecular orbitals were calculated for various metal complexes using Gauss-Sum3, shown in Figure 8. The calculation exhibits significant contributions from the d-orbitals of Co, Ni, Fe, Pt, and Ru near the Fermi level, indicating strong metal–ligand electronic coupling. The analysis of HOMO–LUMO energy gaps provides insight into charge transfer interactions, which affect chemical and electrical reactivity. Contrarily, Zn shows a greater energy gap and weaker interactions due to its filled d^{10} structure, while Cu partially filled d-orbitals result in intermediate behavior. The findings illustrate the variations in electronic structure, charge loss, and potential chemical activity among the metal centers studied.

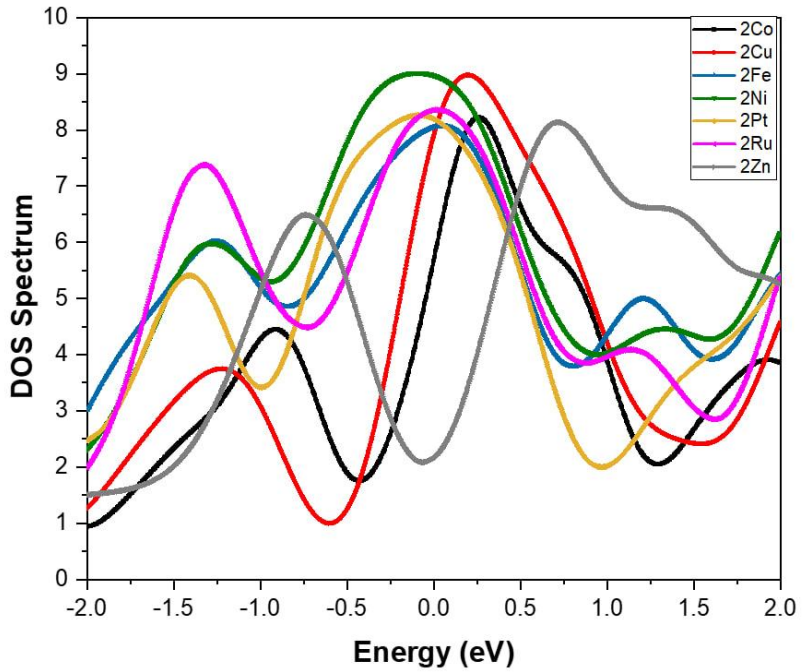

Figure 8: The DOS of the diatomic metal complex molecules for: (Co, Cu, Fe, Ni, Pt, Ru, Zn).

3.2 Optical properties

3.2.1 Ultraviolet spectrum

Figure 9 shows the UV spectra using the TD-DFT analysis with the B3LYP functional and LanL2DZ basis set. The calculation reveals a varied absorption spectrum for the metal–ligand complexes studied. The platinum complex exhibited the highest absorbance around (700 nm), indicative of a strong charge-transfer transition. In contrast, the cobalt complex displayed a weaker peak in the (815–825 nm) range, suggesting strong metal–ligand interactions, while the iron and nickel complexes had modest absorbance at approximately (760 nm) and (630 nm), respectively. The ruthenium complex showed a weaker band around (820 nm), and the copper complex had a distinct peak near (540 nm). The zinc compound exhibited minimal absorption around (460 nm). These variations in absorption characteristics are attributed to differences in central metal ions and their coordination environments, influencing d-orbital configurations and charge-transfer properties.

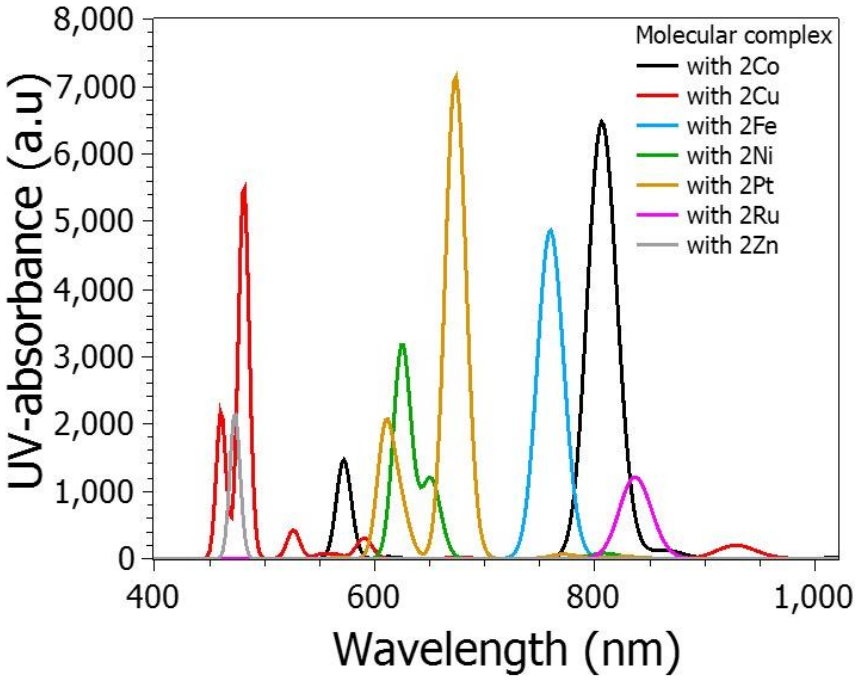

Figure 9: TD-DFT/B3LYP calculation of UV spectrum vs the Wavelength.

3.2.2 IR spectrum

Using the DFT/B3LYP method with the LanL2DZ basis set, the IR absorption spectra of seven diatomic metal complexes coordinated with varied metal atoms shown in Figure 10 were computed. The IR spectra identified key vibrational bands, with a notable absorption around (880–903 cm^{-1}) indicating intact aromatic C–H bending vibrations post-coordination. Bands emerged between (1043 and 1141 cm^{-1}) representing stretching modes C–C and C–F, revealing slight electronic changes. The conjugated π-system showed C=C and C=N stretching from (1575–1631 cm^{-1}) with small shifts in selected complexes suggesting π-back donation from metal centers. The C—C stretching in the alkyne region (2282 to 2303 cm^{-1}) displayed variations based on ligand-metal interactions. Zn(II) and Co(II) complexes yielded distinctive bands, while overall spectral analysis confirmed effective coordination without structural integrity compromise, demonstrating DFT utility in examining vibrational properties in metal-ligand complexes.

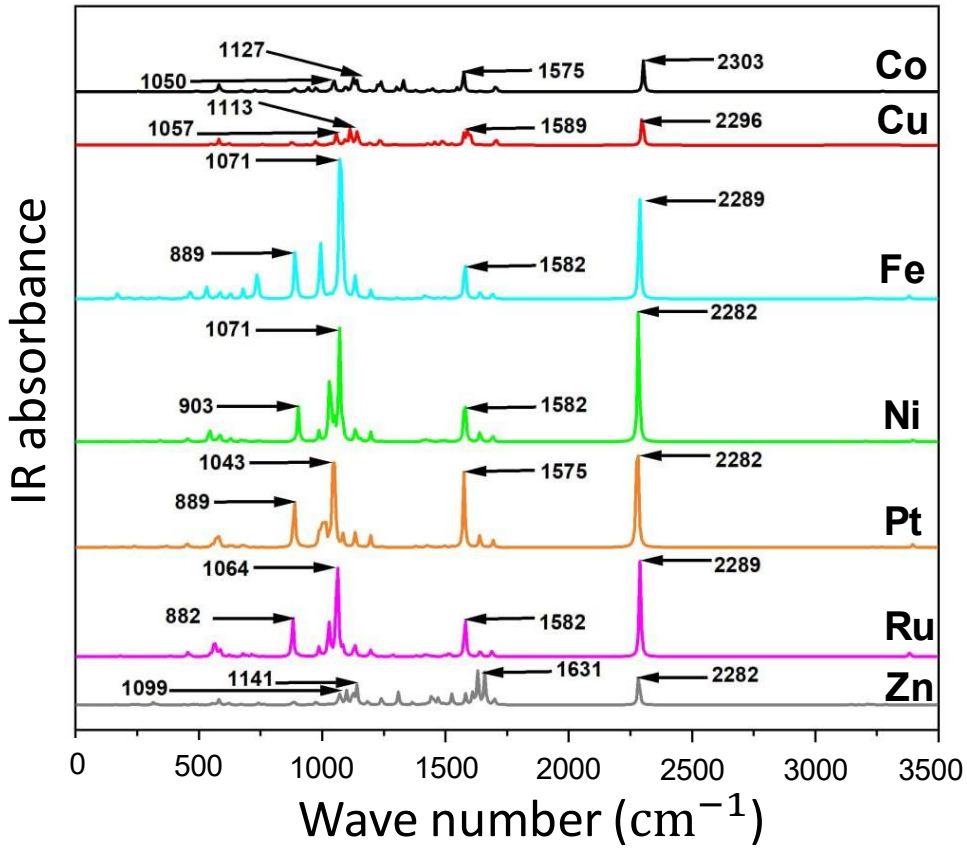

Figure 10: The DFT/B3LYP calculation of IR absorbance spectra of dinuclear complex molecules.

3.3 Interaction and Gibbs Free Energies of the metal Complex

Table 2. Summary of Interaction Energies ($\Delta E_{(Int + ZPE)}$) and Gibbs Free Energy (ΔG) for dinuclear complexes with Co, Cu, Fe, Ni, Pt, Ru and Zn.

Complexes	$\Delta E_{(Int + ZPE)}$ (eV)	ΔG (eV)
Co	-6.24	-5.62
Cu	-4.31	-3.65
Fe	-8.31	-7.58
Ni	-8.79	-7.80
Pt	-9.96	-8.96
Ru	-7.85	-6.98
Zn	-6.06	-5.61

Table 2 shows the calculated thermodynamic analysis, including interaction energies between the two metals and the host of ligand. In all studied dinuclear complexes, the sign of interaction energies are negative, which predict that the doped molecule with each metal thermodynamically a feasible process. The calculation demonstrates that the higher interaction is seen for Pt-dinuclear complex (- 9.96 eV) followed by Ni (-8.79 eV), Fe (-8.31 eV) and Ru (-7.85 eV) complexes, which exhibit the thermodynamic stability of these metallo-dinuclear molecules. The highest magnitude of interaction energy for Pt- dinuclear complex is strongly associated with the lower metal-ligand bond. Furthermore, Gibbs free energy (ΔG) of interaction is calculated to quantify the entropic effects by using Eq 8. The Gibbs free energy calculation reveals the same trend in the interaction energies. The higher ΔG is obtained for Pt- dinuclear complex (-8.96), followed by Ni (-7.8), which refers a similar trend of the thermodynamic stability of these dinuclear complexes as found for electronic interaction energies.

In general, the results for the interaction energies are found in the range of -4.31 eV to - 9.96 eV for all cases of metals. In the case of Fe, metallo- dinuclear molecule exists more commonly as F(III) in the presence of counter anion. Therefore, we have also calculated the interaction and Gibbs free energies for dinuclear molecule complexed with Cl- counter ion (see Figure 3). The resulting interaction and Gibbs free energies are shown in Table 3 reveals that in the presence of counter anion, the energy interaction is remarkably increased to -24.45 eV and -24.23, which leads to higher thermodynamic stability.

Table 3. Comparison of interaction and Gibbs free energies for the dinuclear molecule with Fe and Fe with counter ion Cl^-.

Complexes	$\Delta E_{(Int + ZPE)}$ (eV)	ΔG (eV)
Fe	-8.31	-7.58
Fe-Cl^-	-24.45	-24.23

4. Conclusions

To conclude, we have used B3LYP-density functional theory to study the electronic, optical and thermodynamic properties of the dinuclear transition-metal complexes chosen from the family of metals Co, Cu, Fe, Ni, Pt, Ru and Zn. We found that the

formation of metal complex significantly tunes the electronic, optical properties. The calculated frontier molecular orbitals of varied coupled centers of metals exhibit different occupations of the orbitals, leading to alter the HOMO–LUMO energy gap in the range 0.27 to 2.06 eV for Ni- and Co-complexes. The large energy gap means it is energetically unfavorable to add an electron to the high-energy Lowest Unoccupied Molecular Orbital (LUMO) or to remove one from the low-energy Highest Occupied Molecular Orbital (HOMO) [30]. The larger ionization potential versus the smaller electron affinity were obtained in the case of Cu (IP = 6.74 eV and EA = 2.83 eV), while the case of Fe reveals the lowest value of IP = 3.38 eV and the highest value of EA = 7.78 eV. The opposite relationship between energy gap and reactivity is supported by global hardness, where Co has the highest hardness (η = 1.03) and Ni has the lowest hardness (η = 0.13) and highest softness (S = 7.27). Whereas, the molecule with Fe atom reveals the electronegativity (χ = 6.04 eV).

This discrepancy is explained by the fact that Zn, with its fully filled d^{11} structure, lacks accessible orbitals for further electronic interactions, whereas with Fe is partially filled *d*-orbitals efficiently stabilize incoming electrons through strong metal–ligand interactions. The chemical potential values further support this trend: Zn exhibits the least negative value (μ = −4.33 eV), indicating a smaller electron-attracting capacity, while Fe exhibits the largest negative value (μ = −6.04 eV), showing an important thermodynamic attraction for electron absorption [31].

Due to asymmetric charge distribution and significant polarization, the molecule with Cu exhibits the highest value of the dipole moment (~4 Debye), which directly reflects this electrical characteristic. On the other hand, the molecule with Ni complex has the lowest dipole moment (~1.8 Debye), which is comparable with its small energy gap and strong reactivity as well as a more symmetric electron distribution and faster charge redistribution.

The strong *d*-orbital contributions close for the Fermi level in the DOS analysis show that Co, Fe, Pt, and Ru complexes have the highest level of electron delocalization from an orbital and transport perspective, resulting to improved charge transport characteristics. Zn, on the other hand, provides most because of its closed-shell

structure, which results in a confined electron density and inefficient transport behavior [32].

This electronic structure dependence directly extends to optical properties, where the Pt complex exhibits the strongest absorption (~700 nm), while Zn shows the weakest absorption (~460 nm). significant orbital overlap and relativistic effects facilitate effective metal-to-ligand charge transfer (MLCT) transitions, which are responsible for Pt significant absorption, while Zn full d-orbitals prevent such transitions. The *d*-electron configurations of other complexes (Co ≈820 nm, Fe ≈760 nm, and Ni≈630 nm) control their intermediate absorption behavior. These correlations stem from differences in the metal-ligand coupling strength, orbital hybridization, and *d*-electron configuration, that when combined control the complexes optoelectronic performance, stability, reactivity, and charge transport [33].

In addition to the thermodynamic study, all dinuclear complexes have negative Gibbs free energies (ΔG) and interaction energies (ΔE_{int}), showing that their production is spontaneous and thermodynamically advantageous. The results show that the Pt complex has the higher negative interaction energy (ΔE_{int} = −9.96 eV) and Gibbs free energy (ΔG = −8.96 eV), while the Cu complex has the lower (ΔE_{int} = −4.31 eV and ΔG = −3.65 eV), indicating that the Pt complex exhibits the highest thermodynamic stability due to strong metal–ligand interactions resulting from efficient d-orbital overlap and enhanced orbital hybridization, which increase binding strength and stabilize energy. On the other hand, The Cu complex has the lowest stability due to lower metal–ligand interactions as well as decreased effective orbital overlap, which lead to a lower binding strength [34, 35].

In the presence of the counter ion Cl^-, the interaction and Gibbs free energies for the iron-based complex (Fe-Cl^-) change from ΔE_{int} = −8.31 eV and ΔG = −7.58 eV to ΔE_{int} = −24.45 eV and ΔG = −24.23 eV. Enhancing the electrical interactions and better charge balance within the complex are responsible for this significant decrease, which shows a strong improvement in thermodynamic stability. The stronger binding and a more favorable formation process are indicated by higher thermodynamic stability, which is generally correlated with more negative ΔE_{int} and ΔG. This provides the guidelines for tailoring optoelectronic properties through strategic metal selection in coupled metal-centre systems.

Acknowledgements

The authors acknowledge the Iraqi Ministry of Higher Education and Scientific Research and University of Al-Qadisiyah for the support.

References

[1] K. Kadota, T. Chen, E. L. Gormley, C. H. Hendon, M. Dincă, and C. K. Brozek, "Electrically conductive [Fe 4 S 4]-based organometallic polymers," *Chemical Science,* vol. 14, pp. 11410-11416, 2023.

[2] S. A. Fitzgerald, X. Xiao, J. Zhao, P. N. Horton, S. J. Coles, R. C. Knighton*, et al.*, "Organometallic platinum (ii) photosensitisers that demonstrate ligand-modulated triplet-triplet annihilation energy upconversion efficiencies," *Chemistry–A European Journal,* vol. 29, p. e202203241, 2023.

[3] G. M. Curtin and E. Jakubikova, "Extended π-conjugated ligands tune excited-state energies of iron (II) polypyridine dyes," *Inorganic Chemistry,* vol. 61, pp. 18850-18860, 2022.

[4] H. Xu, R. Chen, Q. Sun, W. Lai, Q. Su, W. Huang*, et al.*, "Recent progress in metal–organic complexes for optoelectronic applications," *Chemical Society Reviews,* vol. 43, pp. 3259-3302, 2014.

[5] R. H. Crabtree, *The organometallic chemistry of the transition metals*: John Wiley & Sons, 2026.

[6] M. J. Białek, K. Hurej, H. Furuta, and L. Latos-Grażyński, "Organometallic chemistry confined within a porphyrin-like framework," *Chemical Society Reviews,* vol. 52, pp. 2082-2144, 2023.

[7] K. Kadish, K. M. Smith, and R. Guilard, *The Porphyrin Handbook, Volume 3* vol. 3: Elsevier, 2000.

[8] S. Fite and Z. Gross, "Data-Driven Insights into Porphyrin Geometry: Interpretable AI for Non-Planarity and Aromaticity Analyses," *Journal of Chemical Information and Modeling,* vol. 65, pp. 4403-4411, 2025.

[9] T. D. Lash, "Coordination chemistry of modified porphyrinoid systems," *Chemical Reviews,* vol. 122, pp. 7987-7989, 2022.

[10] Y. Zheng, S. Jiang, M. Liu, Z. Yu, Y. Ma, G. A. Solan*, et al.*, "High molecular weight PE elastomers through 4, 4-difluorobenzhydryl substitution in symmetrical α-diimino-nickel ethylene polymerization catalysts," *RSC advances,* vol. 12, pp. 24037-24049, 2022.

[11] A. Forni, D. Malpicci, E. Lucenti, L. Zecchinello, A. Colombo, and E. Cariati, "Recent advances in mono-and multi-nuclear photoluminescent Cu (I) complexes with nitrogen containing ligands and their stimuli responsiveness," *Chemical Science,* 2025.

[12] S. F. Kainat, M. B. Hawsawi, E. U. Mughal, N. Naeem, A. M. Almohyawi, H. M. Altass*, et al.*, "Recent developments in the synthesis and applications of terpyridine-based metal complexes: a systematic review," *RSC advances,* vol. 14, pp. 21464-21537, 2024.

[13] M. Paredes, D. Poveda, P. González-Herrero, and Á. Vivancos, "Bimetallic platinum (ii) complexes with bridging di-NHC and N^ C^ C ligands: synthesis and photophysical properties," *Dalton Transactions,* vol. 54, pp. 15745-15753, 2025.

[14] D. A. Shultz, R. Stephenson, and M. L. Kirk, "Dinuclear ligand-to-ligand charge transfer complexes," *Dalton Transactions,* vol. 52, pp. 1970-1976, 2023.

[15] A. Farokhi, S. Lipinski, L. M. Cavinato, H. Shahroosvand, B. Pashaei, S. Karimi*, et al.*, "Metal complex-based TADF: design, characterization, and lighting devices," *Chemical Society Reviews,* 2025.

[16] A. M. May and J. L. Dempsey, "A new era of LMCT: leveraging ligand-to-metal charge transfer excited states for photochemical reactions," *Chemical Science,* vol. 15, pp. 6661-6678, 2024.

[17] H. C. Fitzhugh, J. W. Furness, M. R. Pederson, J. E. Peralta, and J. Sun, "Comparative Density Functional Theory Study of Magnetic Exchange Couplings in Dinuclear Transition-Metal Complexes," *Journal of Chemical Theory and Computation,* vol. 19, pp. 5760-5772, 2023.

[18] C. J. Cramer, *Essentials of computational chemistry: theories and models*: John Wiley & Sons, 2013.

[19] G. Li, D. Zhu, X. Wang, Z. Su, and M. R. Bryce, "Dinuclear metal complexes: multifunctional properties and applications," *Chemical Society Reviews,* vol. 49, pp. 765-838, 2020.

[20] J. Zhang, A. M. Kuznetsov, I. G. Medvedev, Q. Chi, T. Albrecht, P. S. Jensen*, et al.*, "Single-molecule electron transfer in electrochemical environments," *Chemical reviews,* vol. 108, pp. 2737-2791, 2008.

[21] L. Getzner, D. Paliwoda, L. Vendier, L. M. Lawson-Daku, A. Rotaru, G. Molnár*, et al.*, "Combining electron transfer, spin crossover, and redox properties in metal-organic frameworks," *Nature Communications,* vol. 15, p. 7192, 2024.

[22] M. M. Khalaf, H. M. Abd El-Lateef, M. Gouda, A. A. Abdelhamid, A. A. Amer, and A. Abdou, "Designing, characterization, DFT, biological effectiveness, and molecular docking analysis of novel Fe (III), Co (II), and Cu

(II) complexes based on 4-Hydroxy-2 H-pyrano [3, 2-c] quinoline-2, 5 (6 H)-dione," *ACS omega,* vol. 9, pp. 6466-6481, 2024.

[23] E. Louis, E. San-Fabián, M. A. Díaz-García, G. Chiappe, and J. A. Vergés, "Are electron affinity and ionization potential intrinsic parameters to predict the electron or hole acceptor character of amorphous molecular materials?," vol. 8, ed: ACS Publications, 2017, pp. 2445-2449.

[24] G. Mustafa, I. Shafiq, Q.-u.-a. Shaikh, A. Mustafa, R. Zahid, F. Rasool*, et al.*, "Quantum chemical exploration of A− π1–D1–π2–D2-type compounds for the exploration of chemical reactivity, optoelectronic, and third-order nonlinear optical properties," *ACS omega,* vol. 8, pp. 22673-22683, 2023.

[25] Y. Pavani, S. Aravind, K. Padmavathi, M. Subba Rao, and N. S. Babu, "Solvent dependent structural, electronic, and optical properties of ureidopeptidomimetics: a DFT and TD-DFT study on the effects of donor and acceptor functional groups," *Oxford Open Materials Science,* vol. 5, p. itaf001, 2025.

[26] S. Wagner, F. Kisslinger, S. Ballmann, F. Schramm, R. Chandrasekar, T. Bodenstein*, et al.*, "Switching of a coupled spin pair in a single-molecule junction," *Nature nanotechnology,* vol. 8, pp. 575-579, 2013.

[27] S. Sarfaraz, M. Yar, A. Hussain, A. Lakhani, A. Gulzar, M. Ans*, et al.*, "Metallofullerenes as robust single-atom catalysts for adsorption and dissociation of hydrogen molecules: A density functional study," *ACS omega,* vol. 8, pp. 36493-36505, 2023.

[28] V. T. Hoa, "Density functional theory insights into the solvent effect on the binding energies of Cd 2+ in functionalized MOFs," *RSC advances,* vol. 15, pp. 46649-46663, 2025.

[29] C. A. O'Keefe, K. E. Johnston, K. Sutter, J. Autschbach, R. Gauvin, J. Trebosc*, et al.*, "An investigation of chlorine ligands in transition-metal complexes via 35Cl solid-state NMR and density functional theory calculations," *Inorganic Chemistry,* vol. 53, pp. 9581-9597, 2014.

[30] M. Miar, A. Shiroudi, K. Pourshamsian, A. R. Oliaey, and F. Hatamjafari, "Theoretical investigations on the HOMO–LUMO gap and global reactivity descriptor studies, natural bond orbital, and nucleus-independent chemical shifts analyses of 3-phenylbenzo [d] thiazole-2 (3 H)-imine and its para-substituted derivatives: Solvent and substituent effects," *Journal of Chemical Research,* vol. 45, pp. 147-158, 2021.

[31] M. Franco-Pérez, F. Heidar-Zadeh, P. W. Ayers, F. De Proft, A. Vela, J. L. Gázquez*, et al.*, "Temperature and external fields in conceptual density functional theory," *Chemical Science,* vol. 15, pp. 20090-20121, 2024.

[32] H. Hu, Y. Feng, Z. Wang, L. Zhuo, C. Hu, I. Shakir, *et al.*, "Orbital engineering-activated intrinsic conduction enables ultra-high-rate performance zinc storage in manganese dioxide," *Energy & Environmental Science,* 2026.

[33] G. Morselli, C. Reber, and O. S. Wenger, "Molecular design principles for photoactive transition metal complexes: a guide for “photo-motivated” chemists," *Journal of the American Chemical Society,* vol. 147, pp. 11608-11624, 2025.

[34] M. Dinpajooh, G. L. Hightower, R. E. Overstreet, L. A. Metz, N. J. Henson, N. Govind, *et al.*, "On the stability constants of metal–nitrate complexes in aqueous solutions," *Physical Chemistry Chemical Physics,* vol. 27, pp. 9350-9368, 2025.

[35] O. Gutten and L. Rulisek, "Predicting the stability constants of metal-ion complexes from first principles," *Inorganic Chemistry,* vol. 52, pp. 10347-10355, 2013.